

MountNet: Learning an Inertial Sensor Mounting Angle with Deep Neural Networks

Maxim Freydin, *Member, IEEE*, Niv Sfaradi, Nimrod Segol, Areej Eweida, and Barak Or, *Member, IEEE*

Abstract—Finding the mounting angle of a smartphone inside a car is crucial for navigation, motion detection, activity recognition, and other applications. It is a challenging task in several aspects: (i) the mounting angle at the drive start is unknown and may differ significantly between users; (ii) the user, or bad fixture, may change the mounting angle while driving; (iii) a rapid and computationally efficient real-time solution is required for most applications. To tackle these problems, a data-driven approach using deep neural networks (DNNs) is presented to learn the yaw mounting angle of a smartphone equipped with an inertial measurement unit (IMU) and strapped to a car. The proposed model, MountNet, uses only IMU readings as input and, in contrast to existing solutions, does not require inputs from global navigation satellite systems (GNSS). IMU data is collected for training and validation with the sensor mounted at a known yaw mounting angle and a range of ground truth labels is generated by applying a prescribed rotation to the measurements. Although the training data did not include recordings with real sensor rotations, tests on data with real and synthetic rotations show similar results. An algorithm is formulated for real-time deployment to detect and smooth transitions in device mounting angle estimated by MountNet. MountNet is shown to find the mounting angle rapidly which is critical in real-time applications. Our method converges in less than 30 seconds of driving to a mean error of 4 degrees allowing a fast calibration phase for other algorithms and applications. When the device is rotated in the middle of a drive, large changes converge in 5 seconds and small changes converge in less than 30 seconds.

Index Terms—Deep Neural Network, Inertial Measurement Unit, Inertial Navigation System, Machine Learning, Supervised Learning.

I. INTRODUCTION

INERTIAL sensors are available on most mobile devices and are used in a wide range of applications including navigation [1], [2], motion detection [3], activity recognition [4] and monitoring [5], and other [6]. The inertial measurement unit, sometimes called the motion sensor, measures acceleration and angular velocity in the sensor frame at a rate typically ranging between 100-500 Hz depending on the hardware. Using IMU measurements has two notable properties: (1) the signals are noisy and (2) the acceleration and angular velocity vectors are obtained in the sensor frame. The noise is typically alleviated using classical signal processing methods and problem-specific modelling of the dynamics [7]. However transitioning between different frames of reference requires the relative orientation between frames which is unknown in most cases. In this work, a mobile device with an IMU is fixed to the dashboard of a car as shown in Figure 1 and the

relative orientation between the IMU sensor and the car body is referred to as the mounting angle. More specifically, the problem is formulated such that only the yaw mounting angle is of interest, as shown in Figure 2.

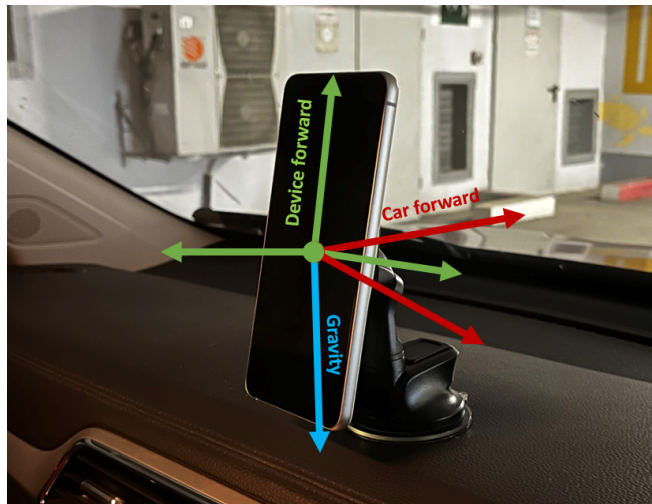


Fig. 1. Smartphone device on a mount inside a car. Sensor data collected by the smartphone is measured in the sensor frame of reference (in green).

Estimating and compensating for the yaw mounting angle of a devices with a built-in IMU sensor is crucial. Indeed, the importance of detecting the IMU mounting angle was noted by several works [8]–[10]. In particular, [10] conducted an experimental study on the effect of a misaligned sensor on the performance of INS/GNSS. Previous attempts to solve the mounting angle detection problem suffer from various ailments. Some methods use only acceleration data, but require a calibration phase where the vehicle is horizontal [11], [12]. In [13] data from motion sensors obtained while the vehicle is turning could not be used. Other approaches do not rely solely on IMU and require additional sensor inputs such as GNSS [14], [15]. In [16] the authors suggest a Kalman filter to estimate the mounting angle using measurements from IMU, GNSS and odometer. Recently, [17] attempted to learn the yaw angle using a synthetic data set generated similarly to this work. However, they used distinctly different machine learning algorithms (an ensemble of regressors) and obtained sub-par results compared to this work.

In previous related work, DNNs were integrated into a wide range of navigation tasks. One of the first works in the field is the robust IMU double integration, the RIDI approach [18], in which neural networks were trained to regress linear velocities from inertial sensors to constrain

Submitted: Dec 2022. This is a preprint version.

All authors are with ALMA Technologies Ltd, Haifa, 340000, Israel (e-mail: {barak,maxim}@almatechnologies.com).

the accelerometer readings. In [19], the device orientation, in addition to the accelerometer and gyroscopes readings, was used as input to a DNN architecture to regress the user velocity in 2D which was then integrated to obtain a position. For land vehicle navigation, a DNN model was presented to overcome the inaccurate dynamics and observation models of wheel odometry for localization, named RINS-W [20]. In [21], recurrent neural networks were employed to learn the geometrical and kinematic features of the motion of a vehicle to regress the process noise covariance in a linear Kalman filter framework. In [22], DNN-based multi-models together with an EKF were proposed to deal with GNSS outages. In [23] it was demonstrated that the integration of DNN into classical signal processing algorithms can boost navigation performance. To the authors' best knowledge, this is the first work to suggest an end-to-end solution based on DNNs to find the yaw mounting angle of an IMU sensor.

In this work, a DNN model with a smoothing algorithm for real-time deployment is developed which receives as input a window of IMU measurements and outputs the estimated sensor yaw mounting angle. A data-driven approach to solve the problem is proposed by collecting recordings of IMU from multiple drives with the IMU sensor strapped to a car at a known yaw mounting angle of zero degrees. To create a rich training dataset, the recorded IMU samples are rotated to simulate a wide range of mounting angles. The model is validated and tested on data with real and simulated rotations. To summarize, the following contributions are made

- 1) A DNN model is designed and trained to estimate the yaw mounting angle of a smartphone fixed to a car using only IMU measurements as input. The training dataset includes more than 52 hours of driving in 136 sessions.
- 2) A method to synthesize ground truth labels is presented and validated. This approach can reduce substantially the data collection effort in future studies.
- 3) An algorithm is formulated to process the DNN output and apply the trained model in real-time.
- 4) The trained model is tested on a validation set consisting of more than 7 hours of driving in 18 sessions. The proposed method is shown to converge in up to 30 seconds to an accurate estimate for the yaw mounting angle with a 4 degrees error.
- 5) An experiment is conducted to test the trained model with the proposed algorithm in a real setting. In addition, results are compared to an existing off the shelf solution which is based on classical fusion of GNSS with IMU.
- 6) The trained model is shown to detect sensor rotation in the middle of the drive at the same speed and accuracy as for the initial angle.

The rest of the paper is organized as follows: Section II presents the data processing and dataset creation. Section III presents the proposed MountNet model architecture and loss function. Section IV presents an algorithm for smoothing and detecting changes in device mounting angle during a drive. Section V gives the results and Section VI presents the conclusions of this work.

II. DATASET CREATION

Data-driven approaches require data collection for offline training and validation of models. In this section, data collection and processing are described.

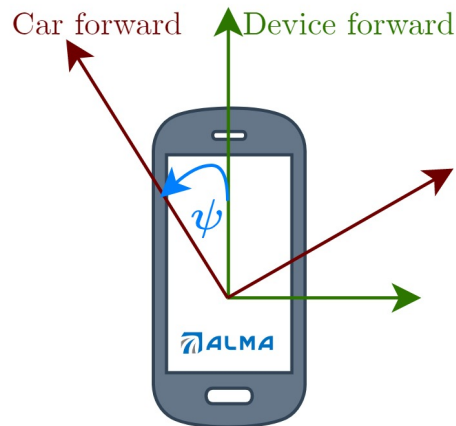


Fig. 2. Top view schematic of the yaw mounting angle, ψ , after adjusting for roll and pitch angles with respect to gravity.

A. Raw data collection

Acceleration and gyroscope data was collected with a WitMotion (WIT) BWT61CL IMU sensor connected to a Windows PC through a serial port connection. Data was recorded in 100 Hz. A total of 60 hours were collected for this task in 154 distinct driving sessions conducted by 4 different drivers in 12 different cities. Of these drives, 136 drives totaling 52.8 hours were used for training and the remainder for validation. The IMU sensor was placed in the same position and orientation on the car dashboard in every drive such that it aligned with the direction of the drive. That is, raw data was collected at a zero mounting angle with a small error due to human factor, i.e., the nominal yaw angle is $\psi = 0 \pm 3$ degrees.

B. Data processing

The collected data consists of acceleration [m/s^2] and angular velocity [rad/s] in three axes. Before passing the data to MountNet, we apply the following pre-processing tasks:

- 1) Apply a low pass filter with a cut-off frequency of 10 Hz. This is justified because the dynamics of a typical car lie in this bandwidth [24].
- 2) Down-sample the data to 20 Hz.
- 3) Rotate the measured acceleration and angular velocity vectors to the navigation frame where the third component is parallel to the gravity vector [7]. This step limits the mounting angle estimation problem to be only a function of the yaw angle as defined in Figure 2. That is, the gravity vector is used to determine the roll and pitch angles, while the car forward direction determines the relative yaw angle.
- 4) Subtract the gravity vector from the third acceleration component.

The above steps are applied offline when training the model and online for using it in real-time. The procedure was designed to simplify the signal and reduce noise and other unnecessary information that is passed to the DNN model.

C. Synthetic datasets creation

As described above, data was collected with the sensor aligned with the car forward direction. To make effective use of the existing data, and reduce human factor errors, the nominal ground truth is always zero degrees. Following the data processing process described in Section II-B, the IMU measurements are independent of the roll and pitch mounting angles, and a synthetic yaw mounting angle can be prescribed.

To create the dataset, recorded drives were partitioned into windows of 5 seconds with a 0.25 seconds overlap. For each window, an angle ψ is drawn from a uniform distribution in the range $[-\frac{3}{4}\pi, \frac{3}{4}\pi]$. This limits the problem to a typical range of mounting angles where the phone screen is facing the inside of the car. The processed IMU measurements window $\mathbf{x} \in \mathbb{R}^{100 \times 6}$ is then rotated by the ψ angle to synthesize a wide range of cases. The acceleration and gyroscope vectors are rotated about the gravity vector by applying a matrix product with

$$\bar{\mathbf{R}}_\psi = \begin{pmatrix} \cos \psi & -\sin \psi & 0 \\ \sin \psi & \cos \psi & 0 \\ 0 & 0 & 1 \end{pmatrix} \quad (1)$$

However, because the acceleration and gyroscope vectors are concatenated, we form the following block matrix,

$$\mathbf{R}_\psi = \begin{pmatrix} \bar{\mathbf{R}}_\psi & \mathbf{0}_{3 \times 3} \\ \mathbf{0}_{3 \times 3} & \bar{\mathbf{R}}_\psi \end{pmatrix}. \quad (2)$$

The matrix product $\mathbf{x}_\psi = \mathbf{x}\mathbf{R}_\psi^T$ rotates the nominal sample \mathbf{x} by ψ to produce the rotated sample \mathbf{x}_ψ . Figure (3) shows an example sample rotation with $\psi = \frac{\pi}{2}$. Four of the six IMU channels (z axis channels are the exception) are changed due to the simulated rotation.

The dataset creation flowchart is shown in Figure 4. The dataset consists of pairs (x_ψ, ψ) where $x \in \mathbb{R}^{100 \times 6}$ is a window consisting of 5 seconds of acceleration and gyroscope readings and $\psi \in \mathbb{R}$ is the simulated mounting angle. The training set consists of 672,858 samples, and the validation set consists of 102,023 samples, keeping a ratio of 85:15 in the train-validation split.

III. MODEL ARCHITECTURE AND TRAINING

Using the data set collected as described above the weights of the MountNet model are trained in a supervised manner. This requires us the definition of a suitable loss function, a specific architecture for the model, and a training regime. In this section, each of these steps is detailed.

A. Loss function

Usually, when dealing with regression tasks DNNs are trained with the mean squared error (MSE) loss. Namely, if

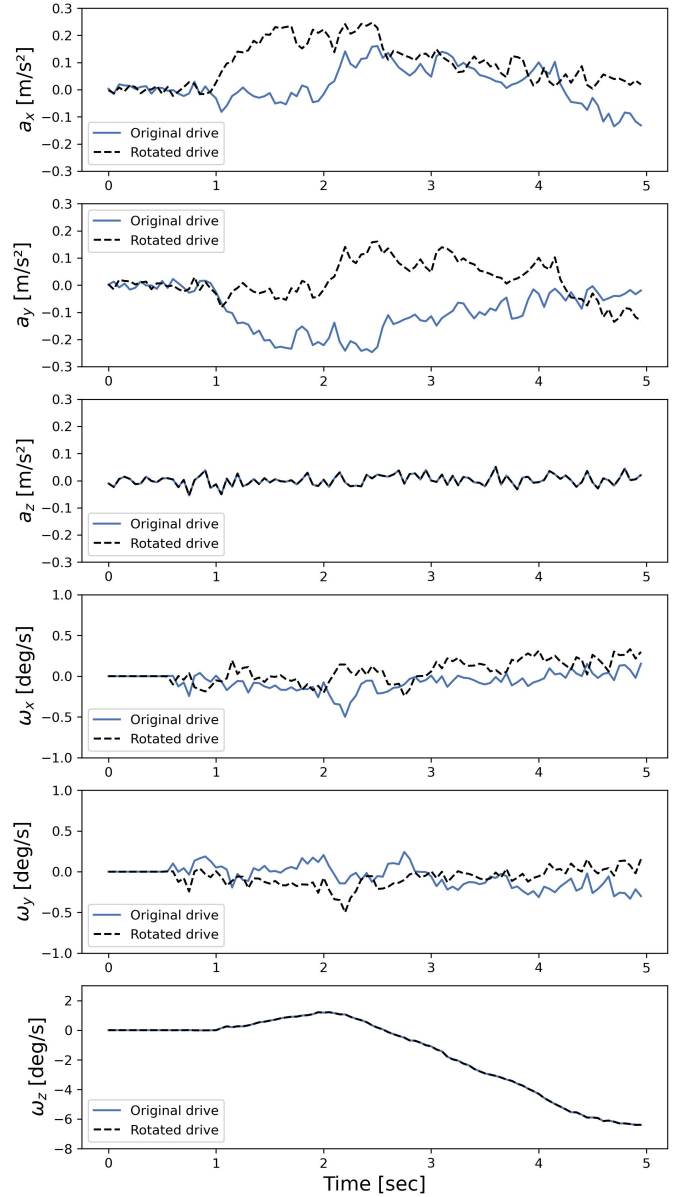


Fig. 3. An example of a single sample in our dataset. We show both x (in dotted black), the 5 seconds of measurement from each of the IMU channels, and $x_{\pi/2}$ (in blue) the same measurements when artificially rotated by an angle of $\pi/2$ about the z axis as described in Section II-C. We can see the effect the rotation has on each of the IMU channels (from top to bottom): acceleration in the x , y , and z axes and angular velocity in the x , y , and z axes.

the output of the CNN is $\tilde{\psi}(x, \mathbf{W})$ where \mathbf{W} are the weights and x is the processed IMU input, then the MSE is,

$$\text{MSE}(\psi, \tilde{\psi}(x, \mathbf{W})) = \frac{1}{2}(\psi - \tilde{\psi}(x, \mathbf{W}))^2. \quad (3)$$

For our purposes, the MSE loss is unsuitable since angles are measured up to a multiple of 2π . For example $\text{MSE}(0, \frac{3}{2}\pi) = \frac{9}{4}\pi^2$, though the squared distance between the angles should be $\frac{1}{4}\pi^2$. To mitigate this issue, a loss function that is similar to the MSE but is agnostic to the periodicity of angles is considered. Specifically, the model is trained with a loss based on the

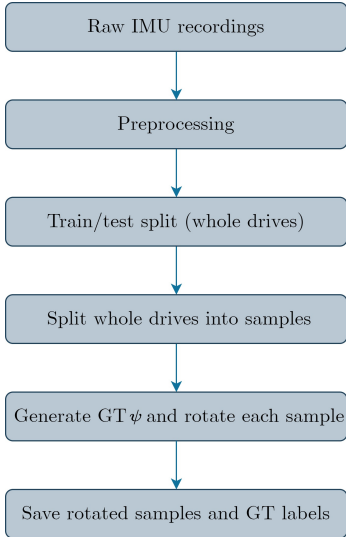


Fig. 4. Data processing and datasets creation flowchart.

function

$$\ell(\psi, \tilde{\psi}(x, \mathbf{W})) = 1 - \cos(\psi - \tilde{\psi}(x, \mathbf{W})). \quad (4)$$

Clearly, this function is periodic, since it is defined using the cosine function. Additionally, the chosen loss approximates the MSE loss in the following way. By Taylor expansion applied to the cosine function, it holds that,

$$\cos(\alpha) = 1 - \frac{1}{2}\alpha^2 + \mathbf{O}(\alpha^4) \quad (5)$$

where \mathbf{O} is the big-O notation. Thus,

$$\begin{aligned} \ell(\psi, \tilde{\psi}(x, \mathbf{W})) &= \\ \text{MSE}(\psi, \tilde{\psi}(x, \mathbf{W})) &+ \mathbf{O}\left(\left(\psi - \tilde{\psi}(x, \mathbf{W})\right)^4\right). \end{aligned} \quad (6)$$

In particular,

$$\ell(\psi, \tilde{\psi}(x, \mathbf{W})) \approx \text{MSE}(\psi, \tilde{\psi}(x, \mathbf{W})). \quad (7)$$

During the training procedure, L_2 regularization with parameter $\lambda = 10^{-6}$ was applied so that the loss reads,

$$\mathcal{L} = \frac{1}{N} \left[\sum_{i=1}^N \ell(\psi_i, \tilde{\psi}(x_i, \mathbf{W})) \right] + \lambda \|\mathbf{W}\|_2^2 \quad (8)$$

where N is the number of samples and ℓ is defined in Equation 7.

B. MountNet Architecture

A convolutional neural network (CNN) architecture was used to solve the regression problem. This allowed the model to capture the temporal information in the IMU signal. the MountNet architecture layers are described here and presented in Fig. 5:

- 1) **Linear layer:** Applies a linear transformation to the input data from the previous layer.
- 2) **Conv1D layer:** A convolutional, one-dimensional (Conv1D) layer creates a convolution kernel that is

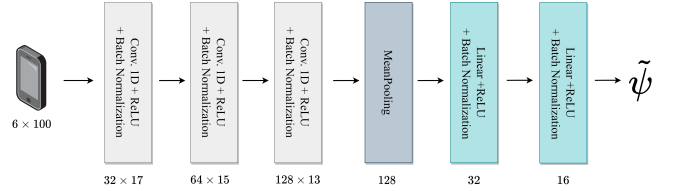


Fig. 5. DNN architecture: three convolutional layers are followed by two dense layers with a connecting mean-pooling layer. The MountNet outputs the mounting angle of the smartphone device inside a car.

convolved with the layer input over a single dimension to produce a vector of outputs. In the MountNet model, the input layer is followed by a chain of three Conv1D layers. The dimensions of the convolutions layers are 32, 64, and 128 with kernel sizes 20, 3 and 3 and stride 5, 1, and 1.

- 3) **Mean pooling:** Pooling layers help with better generalization capability as they perform a down-sampling feature map. For the DNN architecture, we selected the mean pooling method, which calculates the mean value for each input channel and flattens the data so it passes from Conv1D through the linear layers.
- 4) **ReLU:** Rectified linear unit is a nonlinear activation function with the output $ReLU(\alpha) = \max(\alpha, 0)$. The ReLU functions were combined after each layer in the entire MountNet architecture.
- 5) **Batch normalization:** Batch normalization reduces undesirable covariate shift. The batch normalization was added after every Conv1D layer (together with the ReLU layer).

C. Model training

The model consists of 39,905 trainable parameters, which were initialized using Kaiming initialization [25]. We trained the neural network for 1400 epochs using the ADAM optimizer [26] with a learning rate of 0.001, with β coefficients of $\beta_1 = 0.9, \beta_2 = 0.999$, and batch size 128. We trained the model using a Tesla V100 Nvidia GPU. We trained for approximately 14 hours in total, 36 seconds in average per epoch.

IV. REAL-TIME METHOD

The proposed approach is designed for application in real-time. In practice, the output of the MounNet network defined in Section III presents some level of noise. To combat this issue an algorithm was devised to smooth the CNNs output in an online manner. Given a trained MountNet model and continuous input of IMU measurement from a smartphone our algorithm reports the smartphone's mounting angle as the vehicle drives.

At deployment, a window of IMU measurements is passed every half a second through the processing procedure described in Section II-B, and then the processed IMU data at time t , x_t , is fed to the MountNet model. After 5 seconds of initial calibration, the angle output is smoothed using a version

of the well-known $\alpha - \beta$ filter [27]. The filter is formulated by,

$$\hat{\psi}_t = \frac{N-1}{N} \hat{\psi}_{t-1} + \frac{1}{N} \tilde{\psi}(x_t, \mathbf{W}) \quad (9)$$

where $N = \min(30, t)$ is the smoothing window size, $\hat{\psi}_{t-1}$ is the previous output of the algorithm, and $\tilde{\psi}(x_t, \mathbf{W})$ is the output of the MountNet model at time t . We note that as N increases the output of the algorithm becomes smoother but convergence time increases. We found that $N = \min(30, t)$ obtains a good trade-off between convergence time and smoothness, see Figure (6) for a study of different smoothing window sizes.

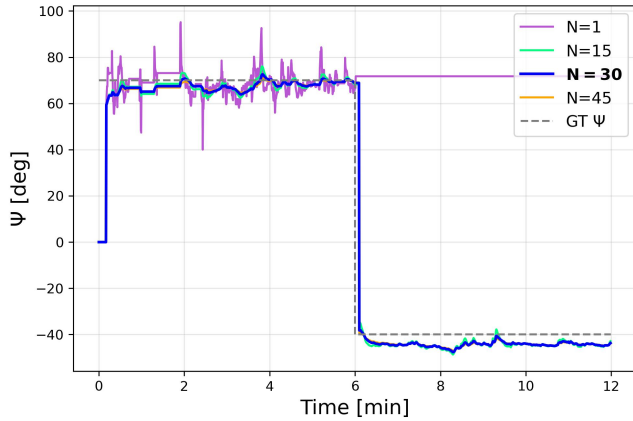


Fig. 6. The result of Algorithm (1) for different values of smoothing window size N . For small smoothing window sizes, the output is noisy and less accurate. Without smoothing ($N=1$), the algorithm treats each output as an outlier and is unable to detect a change in the mounting angle mid-drive. With $N = 45$, results are indistinguishable from $N = 30$, despite the longer run time, justifying the choice of $N = 30$.

A major advantage of the proposed approach is its ability to detect changes in the device’s mounting angle rapidly and in real-time. However, it was found that occasionally the MountNet model reports an angle significantly different than the last reported value even though the mounting angle has not changed. To address this issue, a threshold of $\alpha_T = \pi/6$ is defined to consider angles that differ from the last reported value by more than α_T as outliers.

To handle the case where the angle really does change significantly, the following procedure was added. When the MountNet model reports values that differ from the previously reported mounting angle by more than the threshold for 5 seconds, it is deduced that indeed a change in the mounting angle has occurred and the output of the algorithm is changed accordingly. A full detailed description of the algorithm appears in Algorithm (1).

V. RESULTS

In this section, MountNet performance (accuracy and convergence time) is presented for the validation set and an experiment. The validation set consists of recorded drives not used in the training process, however, a similar rotation synthesis is applied to create rotated samples. Results are presented for a constant rotation angle and for an angle change

Algorithm 1 Real-time algorithm to estimate the mounting angle and detect changes mid-drive. Takes as input the MountNet model $\tilde{\psi}$ with trained weights \mathbf{W} and processed IMU measurements. Continuously outputs $\hat{\psi}_t$ the estimated mounting angle at time t .

```

1:  $ctr\_sec \leftarrow 0$ 
2: for  $t = 0[s], 0.5[s], 1[s], \dots$  do
3:    $x_t \leftarrow$  processed IMU data
4:   if  $t < 5$  then
5:      $\hat{\psi}_t \leftarrow 0$ 
6:      $ctr\_sec \leftarrow ctr\_sec + 1/2$ 
7:   else
8:     if  $ctr\_sec = 5$  then
9:        $ctr\_sec \leftarrow 0$ 
10:       $\hat{\psi}_t \leftarrow \frac{1}{10} \sum_{\tau=t-5}^t \tilde{\psi}(x_\tau, \mathbf{W})$ 
11:    else
12:      if  $\sin(\tilde{\psi}(x_t, \mathbf{W}) - \hat{\psi}_{t-1}) \in (-0.5, 0.5)$  then
13:         $ctr\_sec \leftarrow 0$ 
14:         $N \leftarrow \min(t, 30)$ 
15:         $\hat{\psi}_t \leftarrow \frac{N-1}{N} \hat{\psi}_{t-1} + \frac{1}{N} \tilde{\psi}(x_t, \mathbf{W});$  Eq.(9)
16:      else
17:         $\hat{\psi}_t \leftarrow \hat{\psi}_{t-1}$ 
18:         $ctr\_sec \leftarrow ctr\_sec + 1/2$ 
19:      end if
20:    end if
21:  end if
22: end for

```

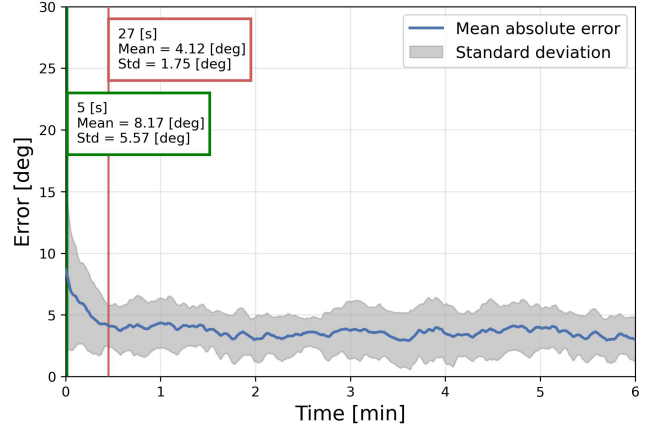


Fig. 7. Estimated mounting angle mean absolute error and standard deviation band vs. time for the validation drives set. The proposed solution achieves a 4.12 degrees MAE after 27 seconds, and 3.5 degrees MAE after 90 seconds.

mid-drive. In addition, results are presented for an experiment with a real rotation of the sensor and MountNet performance is compared to EVK-M8U¹ (by u-blox), an off the shelf positioning product specializing in IMU/GNSS fusion.

A. Evaluation Metrics

We follow the standard evaluation metrics for angle estimation: mean absolute error (MAE) and root mean squared error

¹<https://www.u-blox.com/en/product/evk-8evk-m8> (retrieved on December 2022)

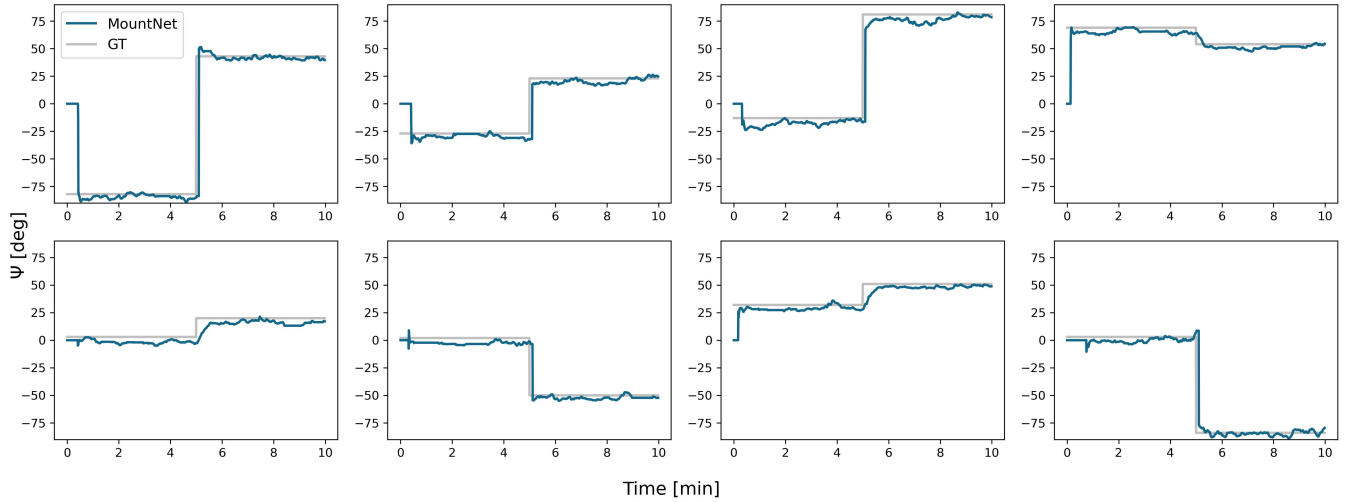


Fig. 8. Estimated mounting angle vs. time with a momentary artificial angle change at $t = 5$ minutes.

(RMSE), as defined in Equation 10 for a set of size \mathcal{M} ,

$$MAE = \frac{1}{\mathcal{M}} \sum_{i=1}^{\mathcal{M}} |\psi_i - \tilde{\psi}_i| \quad (10a)$$

$$RMSE = \sqrt{\frac{1}{\mathcal{M}} \sum_{i=1}^{\mathcal{M}} (\psi_i - \tilde{\psi}_i)^2}. \quad (10b)$$

B. Performance on the validation set

Out of the total 60 hours of recorded data, 7 hours accounted for 18 driving sessions that were not used in the training process. IMU measurements from each of the 18 drives were processed as described in Section II-B and a constant yaw rotation was applied to the full duration of each drive. The prescribed yaw angles were chosen randomly from a uniform distribution in the range of $[-\frac{\pi}{2}, \frac{\pi}{2}]$ radians. Performance metrics are summarized in Tabel I for the raw MountNet output, the smoothed MountNet output using Algorithm 1, and the smoothed output with the first minute of driving removed. The results show that the raw MountNet output is highly noisy as evidenced by the large difference between MAE and RMSE. It is also clear that smoothing improves substantially the accuracy of estimation.

Metric	MountNet	MountNet w/smoothing	MountNet w/smoothing ($t > 1$ min)
MAE [deg]	5.39	3.67	3.53
RMSE [deg]	10.61	4.32	4.09

TABLE I

VALIDATION DATASET PERFORMANCE METRICS FOR MOUNTNET RAW OUTPUT, SMOOTHED OUTPUT USING ALGORITHM 1, AND SMOOTHED OUTPUT WITH THE FIRST MINUTE OF DRIVING REMOVED.

The output time response of MountNet with Algorithm 1 was evaluated on the validation set. Figure 7 shows the mean absolute error, $|\psi_i - \tilde{\psi}_i|$, of the combined algorithm with one standard deviation band versus time. The figure shows the

performance of the combined algorithm during the first six minutes of the 18 validation drives. In the first 30 seconds the output is relatively noisy however the standard deviation reduces rapidly after 15 seconds. The algorithm output error converges to approximately 4 degrees after 27 seconds and 3.5 degrees after 90 seconds of driving. Note that the ground truth data is estimated to have a nominal sensor installation angle error of up to 3 degrees. The run time of the combined algorithm was evaluated on an ASUS PC with Windows 10 and Intel Core i7 processor achieving a 0.5 millisecond per call (a single 5 second input batch).

MountNet performance with Algorithm 1 was evaluated on the validation set with a second synthetic rotation during the drive. In this test, each validation drive is rotated by an additional randomly drawn yaw angle at $t = 5$ minutes. Figure 8 shows the output of the combined algorithm for 8 different drives. In all examples, the output converges near the true angle within 30 seconds of driving. This is true for the initial yaw angle at the drive start and after the angle change. It was observed that convergence after an angle change is reached within 5 seconds for changes greater than $\frac{\pi}{6}$. For smaller angle changes, convergence takes up to 30 seconds and the estimated ψ changes gradually.

C. Experiment results with comparison to an existing solution

So far, MountNet was tested on data recorded with the sensor aligned with the car forward direction and a synthetic yaw rotation. In this section, an experiment is conducted where a real rotation is applied to the sensor. In addition, EVK-M8U by u-blox is used for comparison with an existing solution. EVK-M8U is an evaluation kit that fuses IMU and GNSS for dead reckoning applications in cars. Similarly to a mobile phone device with an IMU, the EVK-M8U is fixed to the car to sense the motion of the car. During its first minutes of operation, in the initialization phase, the u-blox device requires a high-quality GNSS signal to estimate internal parameters which include the yaw mounting angle. Figure 9 shows the

configuration of both devices where the WIT IMU is fixed to and aligned with EVK-M8U.



Fig. 9. Experiment configuration for comparison with existing methods. The u-blox EVK-M8U evaluation device is fixed to the dashboard at near zero roll, pitch, and roll angles. The WIT IMU is fixed to and aligned with the u-blox device.

In the first test drive, the sensors were aligned with the car forward direction as shown in Figure 9 (yaw mounting angle near zero degrees). MountNet was applied with Algorithm 1 and EVK-M8U output was monitored. Figure 10 shows the output of both methods and the ground truth. The first output from EVK-M8U was received 4 minutes into the test with an estimated yaw mounting angle of $\psi = 0.84$ degrees. In the first 30 seconds of the drive, our approach resulted in an estimation error of 10 degrees. Over the whole drive, MountNet achieved an accuracy of 4.4 degrees MAE.

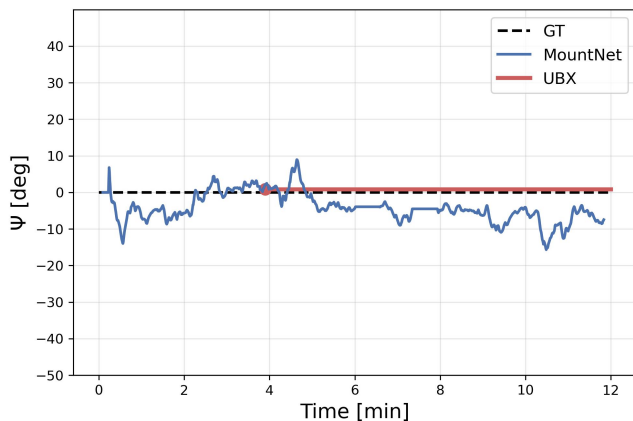


Fig. 10. Estimated mount angle vs. time using MountNet and u-blox. MountNet MAE is 4.4 degrees.

After the first test drive ended, the EVK-M8U finished initialization. The second test drive started with a 3 minutes drive at zero yaw mounting angle followed by a 90 degrees counter-clockwise rotation at $t = 3$ minutes. Figure 11 shows the output from our method and the u-blox device during the second drive. In the first three minutes, both methods agree well, however, at the moment of rotation, the MountNet

responds after 5 seconds to a highly accurate estimation with an MAE of 3.8 degrees while the EVK-M8U takes more than 10 minutes to respond. The final estimation of EVK-M8U converged to 70 degrees with an error of about 20 degrees. In these experiments, MountNet performance was similar to that of the validation set. This supports the use of synthetic rotations (and possibly other operations) to simulate a wide range of sensor installation angles and configurations for training DNN models.

VI. CONCLUSIONS

A data-drive approach was presented for estimating the yaw mounting angle of an IMU sensor. The proposed solution may be used in real-time on mobile devices for navigation, motion tracking, activity recognition, and other tasks. It was shown that the training data can be manipulated to generate a rich set of examples while reducing significantly the data collection effort. The trained model was shown to perform well on a synthetic validation set and in a real setting. The proposed solution is computationally light, easy to deploy, fast to converge, and sufficiently accurate for a wide range of applications. Future and current work include extending the present model to learn the roll, pitch, and yaw mounting angles and apply the presented concepts to other tasks.

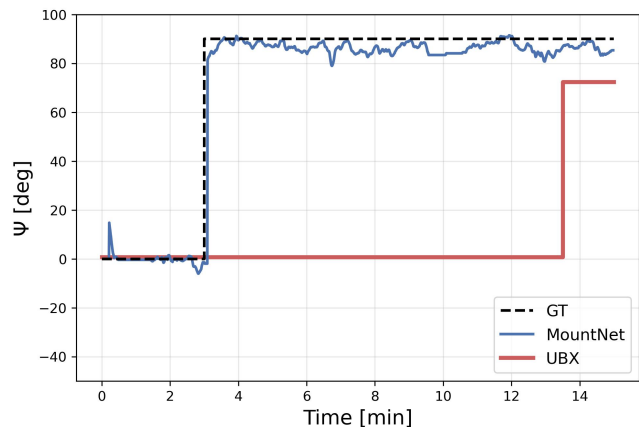


Fig. 11. Estimated mount angle vs. time using MountNet and u-blox with angle change mid-drive. MountNet MAE is 0.8 degrees for the initial angle and 3.8 after the change. After the angle change, MountNet converges within 5 seconds.

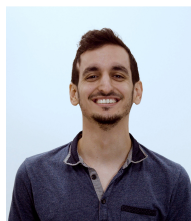
REFERENCES

- [1] G. Dissanayake, S. Sukkarieh, E. Nebot, and H. Durrant-Whyte, "The aiding of a low-cost strapdown inertial measurement unit using vehicle model constraints for land vehicle applications," *IEEE transactions on robotics and automation*, vol. 17, no. 5, pp. 731–747, 2001.
- [2] M. Freydin and B. Or, "Learning car speed using inertial sensors for dead reckoning navigation," *IEEE Sensors Letters*, vol. 6, no. 9, pp. 1–4, 2022.
- [3] T. Seel, J. Raisch, and T. Schauer, "Imu-based joint angle measurement for gait analysis," *Sensors*, vol. 14, no. 4, pp. 6891–6909, 2014.
- [4] S. Ashry, T. Ogawa, and W. Gomaa, "Charm-deep: Continuous human activity recognition model based on deep neural network using imu sensors of smartwatch," *IEEE Sensors Journal*, vol. 20, no. 15, pp. 8757–8770, 2020.
- [5] A. Kashevnik, I. Lashkov, A. Ponomarev, N. Teslya, and A. Gurtov, "Cloud-based driver monitoring system using a smartphone," *IEEE Sensors Journal*, vol. 20, no. 12, pp. 6701–6715, 2020.

- [6] Y. Peng, N. Kondo, T. Fujiura, T. Suzuki, Wulandari, H. Yoshioka, and E. Itoyama, "Classification of multiple cattle behavior patterns using a recurrent neural network with long short-term memory and inertial measurement units," *Computers and Electronics in Agriculture*, vol. 157, pp. 247–253, 2019.
- [7] J. Farrell, *Aided navigation: GPS with high rate sensors*. McGraw-Hill, Inc., 2008.
- [8] S. Hong, M. H. Lee, H.-H. Chun, S.-H. Kwon, and J. L. Speyer, "Experimental study on the estimation of lever arm in gps/ins," *IEEE Transactions on vehicular technology*, vol. 55, no. 2, pp. 431–448, 2006.
- [9] X. Niu and S. Han, "Improving the performance of portable navigation devices by using partial imu based gps/ins integration technology," in *Proceedings of the 21st International Technical Meeting of the Satellite Division of The Institute of Navigation (ION GNSS 2008)*, 2008, pp. 2130–2136.
- [10] Z. F. Syed, P. Aggarwal, X. Niu, and N. El-Sheimy, "Civilian vehicle navigation: Required alignment of the inertial sensors for acceptable navigation accuracies," *IEEE Transactions on Vehicular Technology*, vol. 57, no. 6, pp. 3402–3412, 2008.
- [11] R. C. McKown, "Mounting angle calibration for an in-vehicle accelerometer device," Mar. 21 2017, uS Patent 9,599,633.
- [12] E. Vinande, P. Axelrad, and D. Akos, "Mounting-angle estimation for personal navigation devices," *IEEE Transactions on Vehicular Technology*, vol. 59, no. 3, pp. 1129–1138, 2009.
- [13] H. A. Pham, M. M. Menzel, S. K. P. Chow, and X. Tu, "Detecting mount angle of mobile device in vehicle using motion sensors," Sep. 20 2016, uS Patent 9,448,250.
- [14] J. Cheng, G. Yuan, M. Zhou, S. Gao, C. Liu, H. Duan, and Q. Zeng, "Accessibility analysis and modeling for iov in an urban scene," *IEEE Transactions on Vehicular Technology*, vol. 69, no. 4, pp. 4246–4256, 2020.
- [15] Y. Wu, C. Goodall, and N. El-Sheimy, "Self-calibration for imu/odometer land navigation: Simulation and test results," in *Proceedings of the 2010 International Technical Meeting of The Institute of Navigation*, 2010, pp. 839–849.
- [16] Q. Chen, Q. Zhang, and X. Niu, "Estimate the pitch and heading mounting angles of the imu for land vehicular gnss/ins integrated system," *IEEE transactions on intelligent transportation systems*, vol. 22, no. 10, pp. 6503–6515, 2020.
- [17] E. Bassetti, A. Luciani, and E. Panizzi, "MI-based re-orientation of smartphone-collected car motion data," *Procedia Computer Science*, vol. 198, pp. 237–242, 2022.
- [18] H. Yan, Q. Shan, and Y. Furukawa, "RIDI: Robust IMU double integration," in *Proceedings of the European Conference on Computer Vision (ECCV)*, 2018, pp. 621–636.
- [19] S. Herath, H. Yan, and Y. Furukawa, "Ronin: Robust neural inertial navigation in the wild: Benchmark, evaluations, & new methods," in *2020 IEEE International Conference on Robotics and Automation (ICRA)*. IEEE, 2020, pp. 3146–3152.
- [20] M. Brossard and S. Bonnabel, "Learning wheel odometry and imu errors for localization," in *2019 International Conference on Robotics and Automation (ICRA)*. IEEE, 2019, pp. 291–297.
- [21] B. Or and I. Klein, "Learning vehicle trajectory uncertainty," *arXiv preprint arXiv:2206.04409*, 2022.
- [22] J. Liu and G. Guo, "Vehicle localization during gps outages with extended kalman filter and deep learning," *IEEE Transactions on Instrumentation and Measurement*, vol. 70, pp. 1–10, 2021.
- [23] B. Or and I. Klein, "A Hybrid Model and Learning-Based Adaptive Navigation Filter," *IEEE Transactions on Instrumentation and Measurement*, pp. 1–1, 2022.
- [24] R. Rajamani, *Vehicle dynamics and control*. Springer Science & Business Media, 2011.
- [25] K. He, X. Zhang, S. Ren, and J. Sun, "Delving deep into rectifiers: Surpassing human-level performance on imagenet classification," in *Proceedings of the IEEE International Conference on Computer Vision (ICCV)*, December 2015.
- [26] D. P. Kingma and J. Ba, "Adam: A method for stochastic optimization," *arXiv preprint arXiv:1412.6980*, 2014.
- [27] E. Brookner, "Tracking and kalman filtering made easy," 1998.



Maxim Freydin (Member, IEEE) received his B.Sc. (2017, Summa Cum Laude) and Ph.D. (2021) degrees in Aerospace Engineering from the Technion – Israel Institute of Technology. He is the VP of R&D at ALMA Technologies Ltd. and his research interests include navigation, signal processing, deep learning, and computational fluid-structure interaction.



Niv Sfaradi received his Data Science and Engineering B.Sc. from the Technion - Israel Institute of Technology. He is an algorithm engineer at ALMA Technologies Ltd. and his research interests include deep learning, machine learning, and NLP.



Nimrod Segol received his B.Sc. (2015, Cum Laude) and M.Sc. (2018) degrees in Mathematics from the Technion – Israel Institute of Technology. He is an algorithm engineer at ALMA Technologies Ltd. and his research interests include deep learning, machine learning, and statistics.



Areej Eweida received her B.Sc. (2022) degree in Aerospace Engineering from the Technion – Israel Institute of Technology. She is an algorithm engineer at ALMA Technologies Ltd. She is starting an M.Sc. Her research interests include estimation theory, signal processing, and deep learning.



Barak Or (Member, IEEE) received a B.Sc. degree in aerospace engineering (2016), a B.A. degree (cum laude) in economics and management (2016), and an M.Sc. degree in aerospace engineering (2018) from the Technion–Israel Institute of Technology. He graduated with a Ph.D. degree from the University of Haifa, Haifa (2022). He founded ALMA Technologies Ltd (2021) focusing on Navigation and machine learning algorithms. His research interests include navigation, deep learning, sensor fusion, and estimation theory.